34th Annual International Conference of the IEEE EMBS
San Diego, California USA, 28 August - 1 September, 2012

Modeling the Impulse Response Between Pairs of EMG Signals to Estimate Conduction Delay Distribution

Tahsin Hassan, Kyle C. D. McIntosh, David A. Gabriel and Edward A. Clancy, *Senior Member, IEEE*

***Abstract*— *Mean* electromyogram (EMG) conduction delay is often estimated as the average time delay between two surface EMG recordings arranged along the conduction path. It has previously been shown that the complete *distribution* of conduction delays can be estimated from the impulse response relating the "upstream" EMG recording to the "downstream" recording. In this work, we examined regularized least squares methods for estimating the impulse response, namely the pseudo-inverse with small singular values discarded and post hoc lowpass filtering. Performance was evaluated by training the model to one recording, then testing on others. Correlation between model-predicted EMG and measured EMG was assessed for 36 subjects, using EMG recordings with 5 mm inter-electrode spacing. The best correlation was 0.86, on average, for both regularization methods. We additionally compared the *mean* conduction delay computed from the "gold standard" cross-correlation method to the peak time of the impulse response. The best models differed by 0.01 ms, on average, for both regularization methods. Nonetheless, the impulse responses exhibited excessive energy near zero time, causing delay distribution estimates to exhibit high probabilities at unphysiological short time delays. Inter-electrode spacing larger than 5 mm may be required to alleviate this limitation.**

I. Introduction

Slowed electromyogram (EMG) conduction velocity—often reflected as prolonged delay of an EMG signal propagating between two surface EMG recordings placed along the conduction path—is characteristic in the diagnosis of various myopathic and neurologic conditions [1]–[4]. This slowing is also a well-recognized consequence of localized muscle fatigue [5]–[9]. Numerous methods have been used to estimate mean conduction delay from two conventional surface EMG recordings [10], including: characteristics of spectral dips [11], [12], the delay between reference points in detected waveforms [13]–[16], phase differences [17], maximum likelihood estimation [16], [18], [19], cross-correlation [7]–[9], and the use of double differencing electrodes [8], [16], [20], [21].

Hunter *et al.* [17] modeled the impulse response between the "upstream" EMG recording and the "downstream" EMG recording, assuming that the electrical contributions from individual motor units linearly superimpose, that the action potential shape of each recorded motor unit is identical and that each motor unit action potential is recorded at each electrode site with only a pure (but distinct) time delay. With these assumptions, Williams [22] showed that the *distribution* of delays is directly proportional to the absolute value of the impulse response. Hunter *et al.* used the auto- and cross-spectra of the EMG signals to fashion an estimate of the impulse response, which was demonstrated on one EMG recording using a 15 mm inter-electrode distance. A similar technique was developed by Davies and Parker [23] and demonstrated on one EMG recording using a 20 mm inter-electrode distance.

In this work, we describe a direct method for estimating the impulse response. We model a finite impulse response and use linear least squares to estimate the coefficients of the response. Since least squares is used to solve for the optimal coefficients specifying the impulse response, we examined two methods to regularize the estimate. The first technique uses singular value decomposition to implement the pseudo-inverse, discarding singular vectors whose corresponding singular value is below a threshold fraction of the largest singular value [24]. The second technique smooths the impulse response estimate after completion of the least squares fit. Our techniques were evaluated using data recorded from the tibialis anterior muscle of 36 subjects, using an inter-electrode distance of 5 mm.

II. Methods

A. Experimental Methods

Data from a previous study [25], [26] were reanalyzed. The original study was approved by the Brock University Research Ethics Board and data reanalysis was approved by the WPI Institutional Review Board. All subjects had provided written informed consent.

Subjects lied supine while a 150 mA, constant-current, 1 ms duration, square-wave pulse at a rate of 10 pps was used to find the motor point. The anterior portion of the lower leg was shaved, abraded (NuPrep®, Weaver and Company, Aurora, CO) and cleansed with alcohol. A bar electrode was applied using electrolyte gel (Signa Gel®, Parker Laboratories, Inc., Fairfield, NJ). The recording electrodes on the bar consisted of four stainless-steel tubular surfaces, each 1 mm in diameter and 10 mm long, with an inter-electrode distance of 5 mm. The electrodes were configured to yield three bipolar signals from adjacent electrodes, of which only the first two were utilized (5 mm inter-electrode distance). The ground electrode (CF5000, Axelgaard, Fallbrook, CA) was located on the lateral malleolus. For each experimental session, initial placement was in line with the muscle fibers, between the motor point and the distal tendon of the tibialis

T. Hassan is with The MathWorks (Natick, MA, U.S.A.) and Worcester Polytechnic Institute (WPI), Worcester, MA 01609 U.S.A. (tahsinhassan@gmail.com). E. A. Clancy is with WPI (ted@wpi.edu).

K. C. D. McIntosh (km03ki@badger.ac.brocku.ca) and D. A. Gabriel (dgabriel@brocku.ca) are with Brock University, St. Catharines, Ont., L2S3A1, Canada.

anterior. (This line was marked with indelible ink on the first day.) Electrically evoked potentials were then elicited and the electrode orientation manipulated until electrode placement/orientation maximized action potential shape similarity between EMG channels, as well as delay [19]. Once the electrodes were secured to the skin surface, the impedance was assessed (Grass EZM Electrode Impedance Meter, Astro-Med Inc., Warwick, RI) to ensure that it was lower than 10 kΩ. If not, additional skin preparation was conducted until this criterion was met.

Subjects sat in a testing chair, adjusted so that the hip and knee joints were at 90° and the ankle joint was at 110°. Dorsiflexion forces were applied perpendicular to a load cell (JR3 Inc., Woodland, CA) through an adjustable mount. A padded metal bar secured the top of the foot at the fifth metatarsal. Belts were used to help stabilize the subject within the chair. Subjects then performed three maximal voluntary contractions (MVCs) of the dorsiflexors. The contractions were 5-seconds in duration with a 3-minute rest interval. If subjects were able to reach 110% of the average MVC from these first three trials during a fourth trial, the MVC value was updated to the average of the second through fourth trial. After five minutes rest, 30% MVC trials were conducted. A 30% MVC contraction lasted five seconds, including the force ramp-up period, isometric contraction (2–4 s duration) and the ramp-down period. Only the isometric contraction periods of the 30% MVC trials were utilized in this study. Three 30% contractions, collected over two days, were used in this study. Electrode impedance and skin temperature were again assessed following completion of the last trial. These measures did not change significantly for any subject. The EMG signals were band-pass filtered between 10 and 1000 Hz, amplified (Grass P511, Astro-Med Inc., West Warwick, RI) and sampled with 16 bit resolution at 5000 Hz. The load cell force was also sampled at 5000 Hz.

B. Signal Model and Proposed Solutions

Fig. 1 shows the EMG signal model studied in this work. The noise-free EMG signals are related using convolution as:

$$y[n] = \sum_{i=-p_1}^{p_2} h[i] \cdot x[n-i], \tag{1}$$

where positive integers p_1 and p_2 give the range (in samples) of the impulse response $h[n]$. Integer p_1 produces an impulse response with "system anticipation," which is necessary to fully capture the system dynamics, even when modeling pure time delays [27]. Replacing the noise-free EMG signals with their corresponding measured signal minus their corresponding noise and manipulating gives:

$$v[n] = \sum_{i=-p_1}^{p_2} h[i] \cdot u[n-i] + e[n], \tag{2}$$

where $e[n] = s[n] - \sum_{i=-p_1}^{p_2} h[i] \cdot r[n-i]$, is an error term.

The model in (2) consists of measured upstream signal $u[n]$, measured downstream signal $v[n]$ and the $p_1 + p_2 + 1$ unknown impulse response coefficients $h[n]$ (plus additive noise). With $u[n]$ and $v[n]$ known over a range of samples $N >> p_1 + p_2 + 1$, the coefficients are over-determined and thus can be solved for via least squares estimation [24]. In general, the least squares problem can be ill-conditioned. Thus, two methods of regularization were used. In the first approach, the least squares solution was solved using the pseudo-inverse approach with singular value decomposition. Singular vectors were discarded if their corresponding singular value was less than a specified fraction ("tolerance") of the largest singular value. [This tolerance definition differs from that used in the MATLAB pinv() command.] The following tolerances were examined: 0.9, 0.8, 0.7, 0.6, 0.5, 0.4, 0.3, 0.2, 0.1, 10^{-2}, 10^{-3}, 10^{-4}, 10^{-5} and 10^{-6}. In the second approach, the impulse response was computed using regular least squares, and then the resulting response was lowpass filtered. A 4th-order Butterworth filter was designed, and applied in both the forward and reverse time directions to achieve zero phase. The cutoff frequencies examined were: 25, 50, 75, 100, 125, 150, 175, 200, 225, 250, 275, 300, 325, 350, 400, 450, 500, 600, 850 and 1000 Hz. Such filtering produces start-up transients at both the head and tail of the impulse response. Thus, a more limited (sub-set) range of samples was extracted after filtering, these extents being denoted $p_{1\_Extract}$ and $p_{2\_Extract}$. Since the finite range of the impulse response affects the determined response, we evaluated seven different duration parameter sets, denoted scenarios in Table 1, selected after some initial heuristic evaluation.

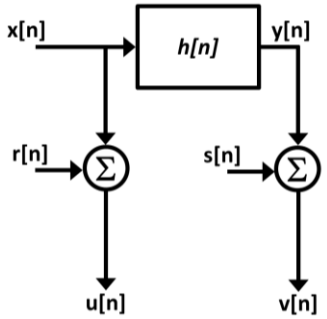

Fig. 1. Model of action potential propagation between ideal "upstream" EMG *x[n]* and ideal "downstream" EMG *y[n]*. Mutually uncorrelated noises *r[n]* and *s[n]* corrupt each signal, producing recorded signals *u[n]* and *v[n]*. Modified from Rababy *et al.*, 1989 [28].

TABLE I

SCENARIOS (PARAMETER SETS) USED TO EVALUATE PERFORMANCE

#	p_1	$p_{1\_Extract}$	p_2	$p_{2\_Extract}$
1	5 ms	4 ms	10 ms	5 ms
2	20 ms	9 ms	20 ms	5 ms
3	16 ms	9 ms	20 ms	5 ms
4	12 ms	5.6 ms	10 ms	5 ms
5	8 ms	4 ms	12 ms	5 ms
6	20 ms	10 ms	20 ms	5 ms
7	0 ms	0 ms	5 ms	5 ms

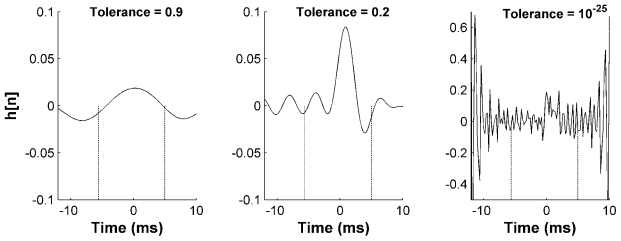

Fig. 2. Sample impulse responses, pseudo-inverse method, scenario 4.

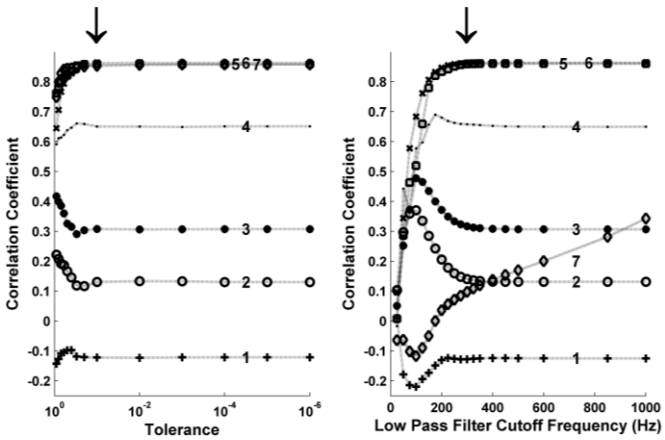

Fig. 3. Average cross-correlation between model-predicted EMG and measured EMG vs. pseudo-inverse tolerance (left) and lowpass cutoff frequency (right). Scenario numbers 1-7 as labeled (see Table 1 for their parameter values). Arrows indicate locations of optimal tolerance/lowpass cutoff frequency.

C. Methods of Analysis

The model was evaluated by training the model to one 30% MVC recording per subject, then testing on the other two recordings. The correlation coefficient between the EMG output estimated by the model and the actual EMG output was used as the performance metric. Mean results are reported (N=72: 36 subjects x two test trials per subject).

In addition, the time location of the peak of the impulse response is an estimate of the *mean* propagation delay. On the two test recordings, the location of this peak was compared to the *mean* delay produced by cross-correlating the upstream and downstream recordings. In both cases, the signals were upsampled to 50 kHz in order to improve the resolution of the peak location. The mean differences are reported (N=72: 36 subjects x two test trials per subject).

III. Results

Fig. 2 shows sample impulse responses. When the tolerance was too low (right), the response was corrupted with high frequency noise. When the tolerance was too high (left), the response was overly smoothed, losing too much shape definition. Similar results were seen with the lowpass filter method of regularization.

Fig. 3 shows the average cross-correlation between the model-predicted EMG and measured "downstream" EMG. In general, as the tolerance value was decreased or the lowpass

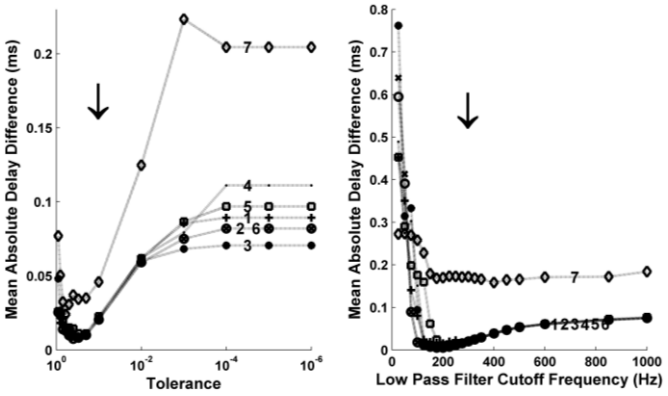

Fig. 4. Average delay absolute difference between "gold standard" cross-correlation approach and peak location of impulse response as a function of pseudo-inverse tolerance (left) and lowpass cutoff frequency (right). Scenario numbers 1-7 as labeled (see Table 1 for their parameter values). Arrows indicate locations of optimal tolerance/lowpass cutoff frequency.

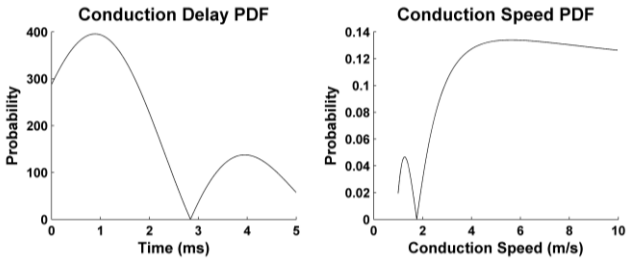

Fig. 5. Estimated conduction delay probability density function (PDF) and conduction speed PDF. Same data and parameters as Fig. 2, middle.

filter cutoff frequency increased, there was an initial stage of transient performance, followed by a long plateau of stable performance. For the best scenarios (5 and 6), the stable stage provided the highest correlation of ≈0.86 for both regularization methods. For the pseudo-inverse approach, the stable stage consisted of all tolerance values below ≈0.2−0.1. For the post hoc filtering approach, the stable stage consisted of all cutoff frequencies above ≈250−300 Hz.

Fig. 4 shows the results comparing the "gold standard" cross-correlation technique of estimating *mean* conduction delay to estimates based on the peak location of the impulse response. The optimal pseudo-inverse tolerance value occurs at ≈0.5–0.2, with acceptable results between 0.7 and 0.1. The optimal post hoc lowpass cutoff frequency occurs at ≈150–200 Hz, although performance drops off somewhat slowly for increasing values. Cutoff frequencies below ≈100 Hz produce exceedingly large errors. At these optimal locations, scenario 7 performed much poorer than all other scenarios. With both methods, the optimal parameters provide an average delay difference of ≈0.01 ms. Typical conduction velocities between 3–5 m/s correspond to delays of 1–1.67 ms using an inter-electrode spacing of 5 mm.

Finally, Fig. 5 shows a sample conduction delay probability density function (PDF) and corresponding conduction speed PDF. The conduction delay PDF is formed as the absolute value of the impulse response, restricted from 0–5 ms and normalized to an area of 1. The conduction speed PDF is derived from the conduction delay PDF. Note the excessive probability at delays near zero (left) and corresponding high speeds (right).

IV. Discussion

Both the pseudo-inverse and lowpass filtering approaches smooth the impulse response estimate. Too little smoothing produces impulse responses with erratic high frequency content; too much smoothing obscures shape discrimination. A pseudo-inverse tolerance value of ≈0.2 or a post hoc lowpass filter cutoff frequency of ≈250 Hz was optimal. In the future, alternative regularization techniques might be considered, such as classical ridge regression or modern multi-scale methods.

Cross-correlation performance is quite sensitive to the time duration used in the estimate. For example, scenarios 2 and 6 are nearly identical, with $p_{1\_Extract}$ differing only 1 ms. Yet, Fig. 3 shows substantial differences in their upstream-downstream correlation (difference of ≈0.8). Contrarily, delay difference performance was quite similar for all scenarios except #7, which performed much poorer. This scenario is the only one that excludes "system anticipation," which is needed to fully capture system dynamics [27]. The best performance was achieved by scenarios 5 and 6.

Regardless of the strong performance noted in the measures above, the middle plot of Fig. 2, along with Fig. 5, show unphysiological conduction delay distribution estimates because our impulse functions included substantial signal power at very low and at negative times. The dominant peak of the impulse response in Fig. 2 had a width of 4 ms, centered near 1 ms. System identification requires an adequate amount of smoothing, else the peak can be difficult to reliably distinguish. But, smoothing spreads the peak. This constraint may be a fundamental limitation imposed by using such a small inter-electrode distance (5 mm). A minimum inter-electrode spacing of 10–15 mm may be required.

V. Conclusion

We analyzed the surface EMG from pairs of bipolar electrodes placed on the tibialis anterior of 36 subjects, using an inter-electrode distance of 5 mm. We modeled the impulse response between the electrodes with a FIR structure using two techniques to regularize the least squares fit (pseudo-inverse and post hoc lowpass filtering). Both regularization methods smoothed the impulse response in a similar manner. Inadequate smoothing led to high frequency interference while excessive smoothing impeded shape discrimination. Optimal smoothing occurred with a pseudo-inverse tolerance value of ≈0.2 or a post hoc lowpass filter cutoff frequency of ≈250 Hz. Nonetheless, the resulting impulse responses included substantive power at very low and negative time delays, causing delay distribution estimates to incorrectly exhibit high probabilities at very short conduction delays. Larger inter-electrode spacing may be required to alleviate this fundamental limitation.

References

[1] Zwarts, Drost and Stegeman, "Recent progress in the diagnostic use of surface EMG for neurological diseases," *J Electromyogr Kinesiol* **10**: 287–291, 2000.

[2] Zwarts and Stegeman, "Multichannel surface EMG: Basic aspects and clinical utility," *Muscle Nerve* **28**: 1–17, 2003.

[3] Blijham, Hengstman, Ter Laak, van Engelen and Zwarts, "Muscle-fiber conduction velocity and electromyography as diagnostic tools in patients with suspected …." *Muscle Nerve* **29**: 46–50, 2004.

[4] Blijham, Ter Laak, Schelhaas, van Engelen, Stegeman and Zwarts, "Relation between muscle fiber conduction velocity and fiber size in neuromuscular disorders," *J Appl Physiol* **100**: 1837–1841, 2006.

[5] Chaffin, "Localized Muscle Fatigue—Definition and Measurement." *J Occup Environ Med* **15**: 346–354, 1973.

[6] Viitasalo and Komi, "Signal characteristics of EMG during fatigue," *Eur J Appl Physiol* **37**: 111–121, 1977.

[7] Naeije and Zorn, "Relation between EMG power spectrum shifts and muscle fibre action potential conduction velocity changes during local muscular fatigue in man," *Eur J Appl Physiol* **50**: 23–33, 1982.

[8] Broman, Bilotto and DeLuca, "A note on the noninvasive estimation of muscle fiber conduction velocity," *IEEE Trans Biomed Eng* **32**: 341–344, 1985.

[9] Zwarts, Van Weerden and Haenen, "Relationship between average muscle fibre conduction velocity and EMG power spectra during isometric contraction, …," *Eur J Appl Physiol* **56**: 212–216, 1987.

[10] Farina and Merletti, "Methods for estimating muscle fibre conduction velocity from surface electromyographic signals," *Med Biol Eng Comput* **42**: 432–445, 2004.

[11] Lindstrom and Magnusson, "Interpretation of myoelectric power spectra: A model and its applications," *Proc IEEE* **65**: 653–662, 1977.

[12] Farina and Negro, "Estimation of muscle fiber conduction velocity with a spectral multidip approach," *IEEE Trans Biomed Eng* **54**: 1583–1589, 2007.

[13] Lynn, "Direct on-line estimation of muscle fiber conduction velocity by surface electromyography," *IEEE Trans Biomed Eng* **26**: 564–571, 1979.

[14] Gydikov, "Spreading of potentials along the muscle, investigated by averaging of the summated EMG," *Electromyogr Clin Neurophysiol* **21**: 525–538., 1981.

[15] Masuda.,Miyano and Sadoyama, "The measurement of muscle fiber conduction velocity using a gradient threshold zero-crossing method," *IEEE Trans Biomed Eng* **29**: 673–678, 1982.

[16] Schulte, Farina, Rau, Merletti and Disselhorst-Klug, "Single motor unit analysis from spatially filtered surface electromyogram signals. Part 2: conduction …," *Med Biol Eng Comput* **41**: 338–345, 2003.

[17] Hunter, Kearney and Jones, "Estimation of the conduction velocity of muscle action potentials using phase and impulse response function techniques," *Med Biol Eng Comput* **25**: 121–126, 1987.

[18] Farina, Muhammad, Fortunato, Meste, Merletti and Rix, "Estimation of single motor unit conduction velocity from surface electromyogram signals detected with …," *Med Biol Eng Comput* **39**: 225–236, 2001.

[19] Farina, Zagari, Gazzoni and Merletti, "Reproducibility of muscle-fiber conduction velocity estimates using multichannel surface EMG techniques," *Muscle Nerve* **29**: 282–291, 2004.

[20] Farina, Arendt-Nielsen, Merletti and Graven-Nielsen, "Assessment of single motor unit conduction velocity during sustained contractions of the tibialis anterior muscle …," *J Neurosci Meth* **115**: 1–12, 2002.

[21] Mesin., Tizzani and Farina, "Estimation of motor unit conduction velocity from surface EMG recordings by signal-based selection of the spatial filters," *IEEE Trans Biomed Eng* **53**: 1963–1971, 2006.

[22] Williams, "Transfer characteristics of dispersive nerve bundles," *IEEE Trans Sys Man Cyber* **2**: 72–85, 1972.

[23] Davies and Parker, "Estimation of myoelectric conduction velocity distribution," *IEEE Trans Biomed Eng* **34**: 365–374, 1987.

[24] Press, Teukolsky, Vetterling and Flannery. Numerical Recipes in C (2nd ed.), Cambridge University Press, New York, 1994, 671–681.

[25] McIntosh. Reliability of Muscle Fibres Conduction Velocity in the Tibialis Anterior. M.S. thesis, Brock University, Canada, 2009.

[26] McIntosh and Gabriel, "Reliability of a simple method for determining muscle fiber conduction velocity," *Muscle Nerve*, **45**: 257–265, 2012.

[27] Hunter and Kearney, "Two-sided linear filter identification," *Med Biol Eng Comput* **21**: 203–209, 1983.

[28] Rababy, Kearney and Hunter, "Method for EMG conduction velocity estimation which accounts for input and output noise," *Med Biol Eng Comput* **27**; 125–129, 1989.